Dynamic spectrum sharing between mobile network operators in GSM

Meghan S. Saitwal

A Dissertation Submitted to

Indian Institute of Technology Hyderabad

In Partial Fulfillment of the Requirements for

The Degree of Master of Technology

भारतीय प्रौद्योगिकी संस्थान हैदराबाद

Indian Institute of Technology Hyderabad

Department of Electrical Engineering

July 2015

Declaration

I declare that this written submission represents my ideas in my own words, and where ideas or words of others have been included, I have adequately cited and referenced the original sources. I also declare that I have adhered to all principles of academic honesty and integrity and have not misrepresented or fabricated or falsified any idea/data/fact/source in my submission. I understand that any violation of the above will be a cause for disciplinary action by the Institute and can also evoke penal action from the sources that have thus not been properly cited, or from whom proper permission has not been taken when needed.

(Signature)

Meghan S. Saitwal
EE12M1029
(Roll No.)

Approval Sheet

This Thesis entitled Dynamic spectrum sharing between mobile network operators in GSM by Meghan S. Saitwal is approved for the degree of Master of Technology from IIT Hyderabad

(Dr. Sumohana Channappayya) Examiner
Dept. of Electrical Eng
IITH

(Dr. P. Rajalakshmi) Examiner
Dept. of Electrical Eng
IITH

(Dr. M. Zafar Ali Khan) Adviser
Dept. of Electrical Engineering
IITH

(Dr. G. V. V. Sharma) Chairman
Dept. of Electrical Eng
IITH

Acknowledgements

The work presented here would not have been possible without the guidance and support of people who in one way or other extended their valuable assistance. I take this opportunity to express my sincere gratitude towards them. First and foremost, I would like to thank my adviser Dr. Mohammed Zafar Ali Khan for his phenomenal valuable guidance and support. I would like to thank my friends for their help at all times.

Dedication

Dedicated to my beloved parents and family...

Abstract

Today's cellular networks are governed by fixed spectrum allocation policy. This allocation is done by spectrum auctioning. The different GSM operators own mutually exclusive spectrum which means one operator can't use other operator's spectrum. This results into an in-efficient use of spectrum which is proved by several measurement studies conducted in different parts of the world.

We addresses the problem of inefficient spectrum utilization in GSM using dynamic spectrum sharing (DSS) between mobile network operators. GSM is used as a case study because it is expected to sustain for 15-20 years in India and other developing countries. The proposed spectrum sharing scheme is evaluated under the different traffic conditions for base stations (BSs). The results for the proposed scheme shows significant improvement in spectrum utilization with reduced call blocking probability. The different DSS schemes are presented for two and three BS co-ordination. New element called as "Spectrum sharing co-ordinator (SSC)" is introduced in system architecture to carry out all spectrum sharing related activities.

Here, we considered SSC is having knowledge of radio resources of all the BSs involved in co-ordination. But, when it is not known, in that case, we need to implement spectrum sensing to identify free resources of BSs. So, we worked on several spectrum sensing techniques also. Energy detection is the simplest and least complex technique, but it requires knowledge of noise power. So, we studied blind spectrum sensing techniques which does not require knowledge of signal to be transmitted and noise. These techniques are dependent on sample covariance matrix of received signal. Test statistics are maximum to minimum eigenvalue (MME) ratio and energy to minimum eigenvalue (EME) ratio. These techniques has very high computational complexity. So, we reduced complexity using upper and lower bounds on eigenvalues and using minimum mean square estimation (MMSE) technique.

Contents

List of Figures

List of Tables

Chapter 1

Introduction

Several measurement studies have proved that spectrum resources are not efficiently utilized [1, 2]. Spectrum occupancy measurements conducted in Mumbai [3] and in South India [4] showed very less spectrum utilization in India. When we observe the spectrum over time period in a particular area, there exists "Spectrum holes". This means that there are many spectrum opportunities that needs to be exploited. The in-efficient use of spectrum is a result of fixed spectrum allocation (FSA) schemes. This is because that the network providers are issued with spectrum licenses for spectrum chunks in an exclusive manner. Therefore, even if one network provider is with free resources at a particular time, other operator is not allowed to use that spectrum.

In order to satisfy increasing service demands with limited number of resources, dynamic spectrum sharing [5, 6, 7, 8, 9] provides a solution to the problem of spectrum under-utilization. Many DSS schemes deal in selling of spectrum licenses for short duration to secondary services which is done generally by primary service or spectrum broker/ server. Spectrum broker pools unused spectrum from MNOs and sells this spectrum on demand basis. Our proposed scheme does not deal with selling of spectrum licenses, but uses other operator's free resources based on own users requirement.

The dynamic spectrum access and spectrum sharing techniques are discussed in [10, 11] for cognitive radio wireless networks. Inter-operator spectrum sharing for UMTS is presented in [12] [13] and the results in [12] showed spectrum efficiency gain of 4% in case when both UMTS operators having same call arrival rates. Different inter-operator resource sharing techniques for 4G LTE cellular networks are discussed in detail in [14]. However, to the best of our knowledge, such a study has not been done in the case of GSM.

We present the simulation results for spectrum sharing between two and three GSM operators. The study shows significant improvement in spectrum utilization, spectrum efficiency gain and call blocking probability. These results are obtained under different traffic conditions for GSM base stations. The base stations of different network providers assumed to be co-located and assumed to be with same coverage area. The results obtained give us an idea on the traffic conditions under which spectrum sharing is beneficial. This allows for smart usage of spectrum according to instantaneous observed traffic.

1.1 Motivation

Cognitive radio is an emerged technology which can improve spectrum utilization by allowing secondary unlicensed users to access primary licensed user's unutilized spectrum. The different spectrum sensing techniques are developed for finding spectrum holes. With the use of this technology, secondary users can use free portion of licensed spectrum without paying anything to licensed user. This is the reason why licensed user will not agree on such use of his spectrum by secondary user.

We present dynamic spectrum sharing scheme between licensed GSM operators rather than allowing secondary users to use free of cost. This will generate an extra revenue for an operator based on the use of his spectrum by other operators. The spectrum usage for GSM operators can be tracked by SSC. Based on tracking done, settlement can be done between GSM operators involved in co-ordination. GSM operators can get economical benefit just by giving its free resources. This fact will attract operators for an implementation of proposed scheme.

1.2 Outline of the thesis

In the present work , we provide a solution to the problem of in-efficient spectrum utilization by sharing spectrum dynamically between MNOs in a particular area under certain traffic conditions. A brief introduction and a extensive literature survey on the problem considered is discussed in Chapter 1.

In Chapter 2, we present newly proposed system architecture for co-ordination between two base stations corresponding to different GSM operators which are co-located. The different DSS schemes with flow graphs are also discussed in this chapter.

Chapter 3 gives simulation results for two and three BS co-ordination by considering all possible traffic conditions. ROC plot for two GSM operators is also given in this chapter.

Spectrum sensing technique based on the eigenvalues of sample covariance matrix with low computational complexity is developed in Chapter 4.

Finally, conclusions and future work is given in Chapter 5.

Chapter 2

System Architecture and Dynamic Spectrum Sharing Schemes

2.1 System Architecture

The system architecture consisting of two GSM operators (OP1 and OP2) with spectrum sharing co-ordinator (SSC) is shown in Fig. 2.1. Both the GSM base stations are connected to the respective mobile switching centres (MSCs) through common SSC.

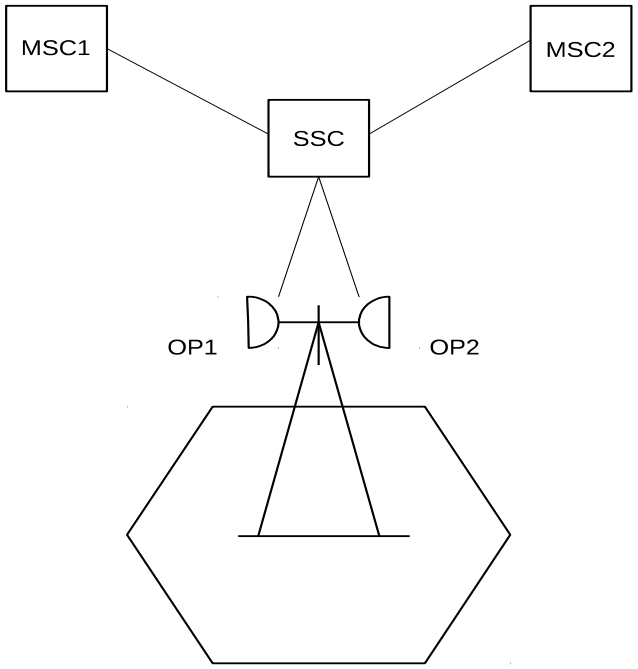

Figure 2.1: Two GSM operators with spectrum sharing co-ordinator.

BS considered here is combination of base transceiver station (BTS) and base station controller (BSC). BTS is an equipment at tower site and BSC is remote device which manages radio resources for BTS. The SSC carries out all the spectrum sharing activities namely user migration between two networks and carrier allocation.

We assume that both the BS are co-located. This is a valid assumption as in many cases the BS locations corresponding to different GSM operators are on same building or tower. These BSs operate at different absolute radio frequency channel numbers (ARFCNs) but with same coverage area. If BTSs are not co-located, then they will having different coverage area. So, we need to consider this in sharing algorithm. It will add complexity and additionally call setup delay; and will be considered in a future study.

The call arrival process is generally modeled as poisson process [15] and call duration parameter can be modeled as exponential, lognormal or Erlang-k distribution [16]. We have assumed that call duration is exponentially distributed.

2.2 Call Setup Analysis

The call establishment procedure involves many steps and these steps are different for shared and non-shared mode. The identified three cases are as follows.

2.2.1 FSA or Non-shared mode

This case refers to standard one as there is no sharing. Users are allowed to camp on their home networks only. In this case, call setup steps include Radio Resource (RR) connection, authentication, alerting, connect, connect acknowledge, etc. The extra signaling messages are not needed through SSC. This is the traditional call setup procedure and is used to compare with non-shared BS mode.

2.2.2 DSA mode with shared BS

In this case, same BS is used to run ARFCN's for both the GSM operators. This case also requires almost same call setup procedure as of non-shared mode. The only difference is with channel allocation procedure i.e. user first tried to accommodate on own ARFCN and then on other. This mode gives same performance results as DSA mode with non-shared BS but with different call setup delays due to the absence of SSC.

2.2.3 DSA mode with non-shared BS

The BSs are not same but they are co-located. The extra signaling messages are needed for re-association if users are not getting accommodated on home network/own operator. This signaling takes place through SSC between two BS and involves an additional call setup delay compared to non-shared mode.

2.3 Dynamic Spectrum Sharing between two GSM Operators

There are different types of spectrum sharing approaches as discussed in [6], [9]. According to the proposed system architecture, there are mainly two approaches i.e. centralized [17], [18] and distributed [19], [20]. The centralized approach controls the allocation of spectrum among the operators with help of spectrum broker. On the other hand, in distributed case, the transmitter chooses channel from available channels with the transmission power. In this paper, we concentrate on centralized sharing between two GSM operators by introducing the entity SSC. Observe that the operators may have coinciding peak hour periods, but different peak loads. So, instantaneous spectrum opportunities can be exploited even during coinciding peak hour due to different call arrivals.

There are many different ways in which we can do dynamic spectrum sharing between two GSM operators. These ways are mainly classified based on the outcome we are expecting from sharing. Most of the papers consider following two parameters:

1. Spectrum Utilization
2. Call blocking probability or Quality of service (QoS)

We also considered same two parameters while designing the sharing algorithm and describe it in context of DSS scheme I as shown in Fig. 2.2. But, when it comes to the practical deployment, the operators will be mainly focusing on the economical benefits from this type sharing. So, while designing spectrum sharing algorithm, we should consider this parameter. From an economical point of view, we can think of several different spectrum sharing techniques based on the charging schemes. The charging scheme is a vital parameter which affects the spectrum sharing algorithm. We further identify two cases i.e. DSS scheme II and DSS scheme III which are discussed in subsection 2.3.2 and subsection 2.3.3 respectively.

In these schemes, an operator is allowed to use only the free resources of another operator. So, for using free resources of another operator, the operator using other operator‘s resources will pay less charges compared to normal call rate. To gain more economical benefit, operator will target to serve own customers preferentially as compared to other operators users. Keeping this in mind, there are two ways of spectrum sharing by considering two new parameters; call handover and QoS.

Each BS is allotted with four ARFCNs and used to transmit GSM frames. Each ARFCN represent a pair of 200 KHz channel with one in uplink and other in downlink. Each GSM frame of duration 4.615ms is divided into eight slots. So, each ARFCN can support seven to eight users/calls by allotting traffic channel (TCH) slots. So, each BS at any time can allow thirty one active calls.

2.3.1 DSS Scheme I

The flowchart in Fig. 2.2 explains DSS Scheme I between two GSM operators. This is the simplest scheme with least complexity without forced handover and call drop. For convenience, new call arrival is considered to OP1 with BS1 in all schemes.

The steps involved in dual-operator GSM spectrum sharing are as follows:

Step 1. A new call arrives at one of the two base stations i.e. BS1 which belongs to OP1.

Step 2. OP1 tries to accommodate the call by allotting free time slot.

Step 3. If call is admitted on own network, then the procedure stops as shown in flowchart in Fig. 2.2.

Step 4. Otherwise, user is transferred to OP2 through SSC. The call will be permitted based on the availability of free resources with OP2 at that particular time.

Step 5. If call is not admitted on OP2 also, then the call will be dropped.

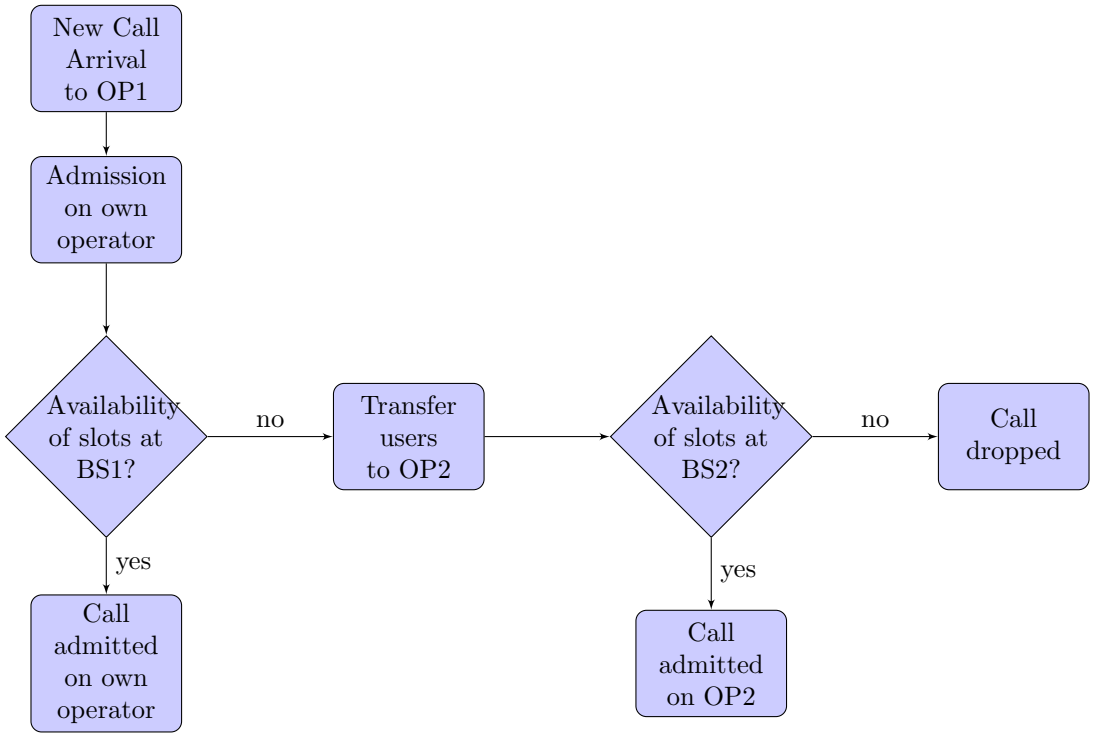

Figure 2.2: DSS Schemem I flowchart

2.3.2 DSS Scheme II

In this scheme, first, a new call will try to occupy TCH at its own operator. If it fails in doing that, it will go to other operator and checks for the availability of free resources. If other operator is also not having any free TCH, then rather than dropping the call like in DSS Scheme I, it will come back to own operator. Now, it will check the occupancy details of own operator. If it is serving other operator users, then one of other operator users will be forced to drop the call. Then, new call will be accommodated on own operator. But, in case, all users with active call are his own, then new call will be dropped.

The steps involved in DSS Scheme II are as follows:

Step 1. A new call arrives at one of the two base stations i.e. BS1 which belongs to OP1.

Step 2. OP1 check for free slots and try to accommodate the call.

Step 3. If call is successfully admitted on own network/ OP1, then the procedure stops as shown in flowchart in Fig. 2.3.

Step 4. Otherwise, user is transferred to OP2 through SSC. The call will be allowed based on free slot availability with OP2 at that time instant.

Step 5. If OP2 also fails in serving call, then user occupancy details of BS1 (of OP1) will be checked.

Step 6. If some of BS1 resources are used by OP2 users, then one of OP2 users will be forced to drop the call and new call of OP1 user will be admitted on own network/ OP1.

Step 7. If only OP1 users are using resources of BS1, then the new call arrived will be dropped.

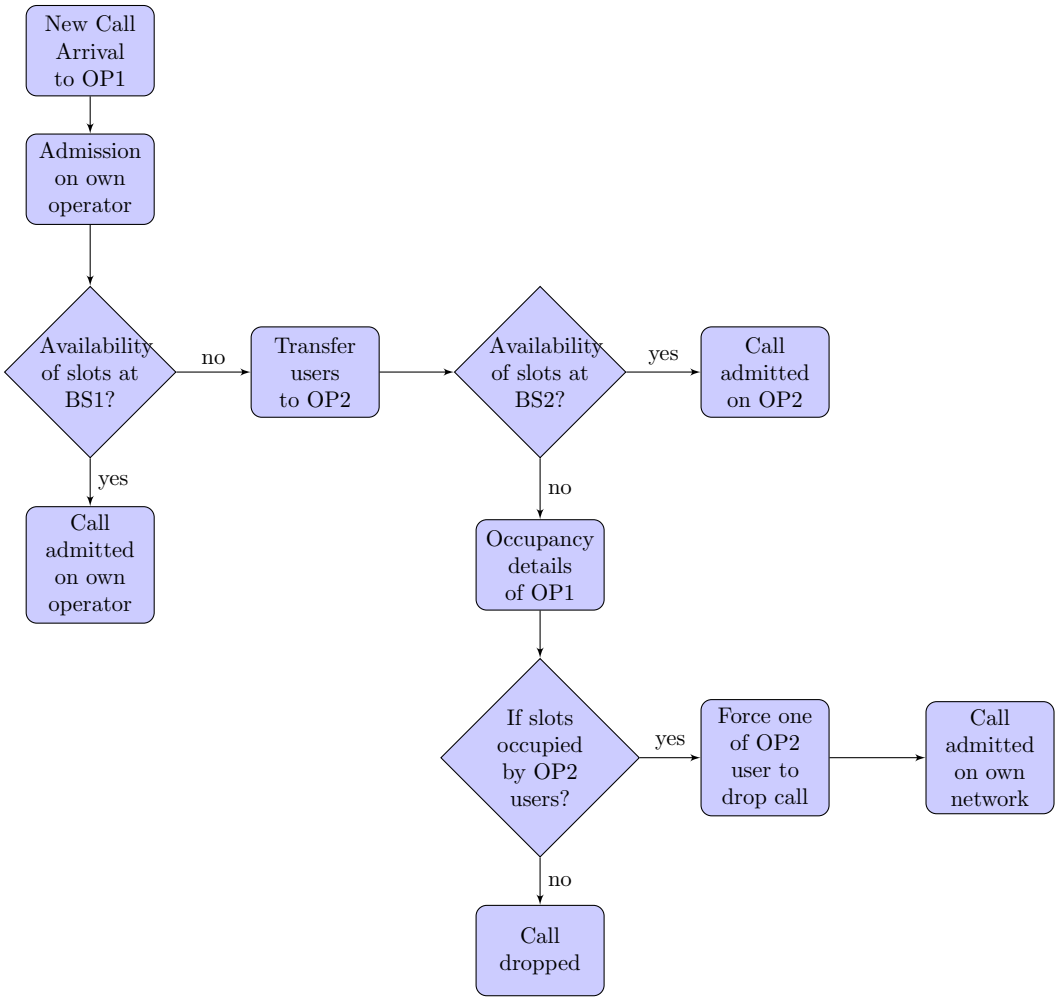

Figure 2.3: DSS Scheme II flowchart

2.3.3 DSS Scheme III

The flowchart for DSS Scheme III is shown in Fig. 2.4. Similar to DSS Scheme I and II, new call will be tried to be accommodated on own operator first. If it is unsuccessful in that, then the occupancy details of own operator will be checked rather than going to other operator as in previous cases. If other operator's users are not using any of resources, then new call will be transferred to other operator and based on availability of free resources, it will be accommodated or dropped.

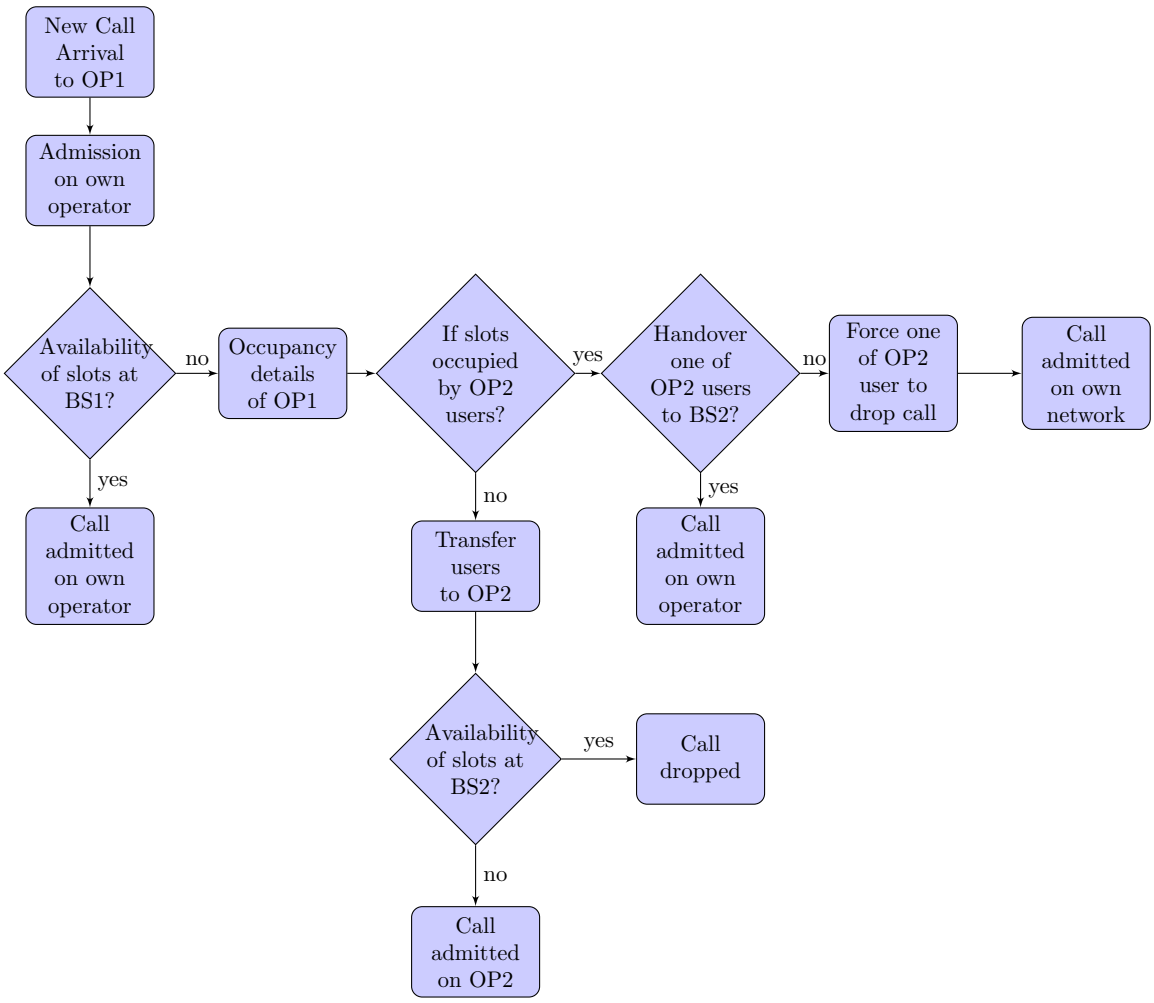

Figure 2.4: DSS Scheme III flowchart

If operator of arrived new call is serving other operator users, then instead of simply dropping one of operator users call, handover attempt will be done. One of other operator's user will be forced to handover the ongoing call to his own operator. If handover fails due to un-availability of resources, then the call will be dropped and finally, new call will be admitted.

The steps involved in DSS Scheme III are as follows:

Step 1. A new call arrives at one of the two base stations i.e. BS1 which belongs to OP1.

Step 2. OP1 tries to serve his own user.

Step 3. If call is admitted on OP1, then the procedure stops as shown in flowchart in Fig. 2.4.

Step 4. Otherwise, user occupancy details of BS1 will be checked. If OP2 users occupied some

resources of BS1, then the following subroutine will be executed.

a. One of OP2 users will opt for handover of call to BS2.

b. If handover is successful, then OP1 user will be admitted on freed resources.

c. In case of failed handover, the ongoing OP2 user call will be dropped and then OP1 user call will be admitted.

Step 5. If only OP1 users are using resources of BS1, then following subroutine is followed.

a. New call arrived at BS1 will be transferred to BS2.

b. If there are free resources with BS2 at that particular time, then call will be admitted on BS2.

c. Otherwise, the call will be dropped.

2.3.4 Comparison of the Three DSS Schemes

DSS Scheme I is the simplest dynamic spectrum sharing technique which involves lower complexity compared to DSS Schemes II and III. Even Scheme I gives exactly same spectrum efficiency gain as other two schemes and call blocking probability is less in this scheme. This is because operator is not giving preference to own customer and not forces other operator user to drop the call. But by doing this, operator looses the economical benefits; in Scheme I. That's why, even if with higher complexity, we consider other two schemes.

DSS Scheme II gives more economical benefit compared to Scheme I but less compared to Scheme III. Because, in Scheme III, new call will not go to other operator even if own operator is busy. Before going to other operator, the occupancy details of own operator will be verified. In terms of QoS, Scheme II outperforms Scheme III, because it does not involve any additional delays due to handovers. The handover considered is not normal handover but it is a forced handover as demonstrated in [21].

2.4 Dynamic Spectrum Sharing between three GSM Operators

The flowchart in Fig. 2.5 explains dynamic spectrum sharing between three GSM operators (OP1, OP2 and OP3). Now, if operator of arrived call is not able to serve, then the call will be transferred to one of two remaining operators involved in co-ordination. To make a choice between two operators, current traffic conditions will be observed at both the base stations corresponding to these operators. Finally, call will be transferred to operator with less traffic load and based on slots availability, call will be admitted or dropped. For convenience, new call arrival is considered to OP1 with BS1.

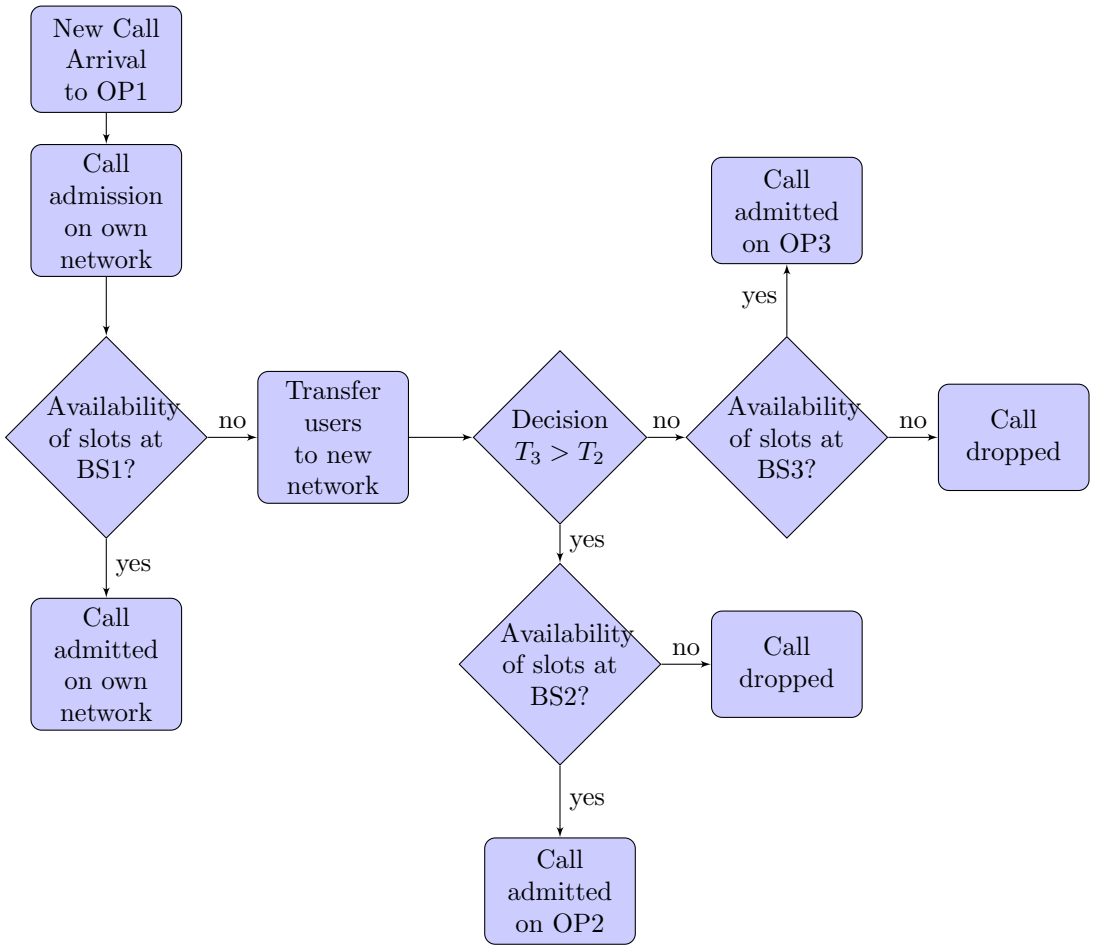

Figure 2.5: Flowchart of Dynamic spectrum sharing between three GSM operators

The steps involved in triple-operator GSM spectrum sharing are as follows:

Step 1. A new call arrives at one of the three base stations i.e. BS1 which belongs to OP1.

Step 2. OP1 tries to accommodate the call by allotting available time slot.

Step 3. If call is admitted on own network, then the procedure stops as shown in flowchart in Fig. 2.5.

Step 4. Otherwise, user will be transferred to OP2 or OP3 through SSC based on the comparison of traffic loads, T2 and T3, of OP2 and OP3.

Step 5. If $T_3 > T_2$, then call will be transferred to OP2. Based on availability of slots at BS2, call will be admitted or dropped.

Step 6. Otherwise, call will be tried to be accommodated on BS3 of OP3.

Chapter 3

Simulation Results

3.1 Simulation Parameters

The MATLAB simulations are done to evaluate the performance of dynamic spectrum sharing between two GSM operators. The simulation parameters are mentioned in Table 3.1. The call arrivals are modeled using the Poisson process with λ as call arrival rate. The call holding times are exponentially distributed with a mean of 120 seconds.

Parameters	**Values**
Service type	Speech traffic
Call Duration	Mean = 120 seconds (Exponential)
Cell radius	1Km
Bandwidth	4 ARFCNs per BS
Call arrival	poisson distributed
Cell layout	Hexagonal with omni-directional antenna
Simulation Interval	1 hour

Table 3.1: Simulation Parameters

Now, we will define terms which will be used in evaluating the performance of spectrum sharing.

1. Spectrum Efficiency, η, is defined as the portion of the spectrum getting utilized per unit time; η can be written as

$$\eta = \frac{\text{Average number of slots utilized per unit time}}{\text{Total number slots available with BS}} \times 100$$

2. Spectrum Efficiency Gain, S_G, is the percentage of spectrum getting more used with the use of spectrum sharing. It can be calculated as the difference between spectrum efficiency with and without the spectrum sharing.

3. Call Blocking Probability, P_B**,** is the probability with which the call is not getting served by base station;

$$P_B = \frac{\text{Number of calls not getting served}}{\text{Total number of calls arrived}}.$$

3.2 2-BS

case I : Call arrival rates are same for both BSs i.e $\lambda_1 = \lambda_2$.

The reason for considering this case is that many times, we observe that during peak traffic hours, call arrival rates for different operators will be same. This case give less gain due to lack of free resources in both the BSs with increasing call arrival rate at same time.

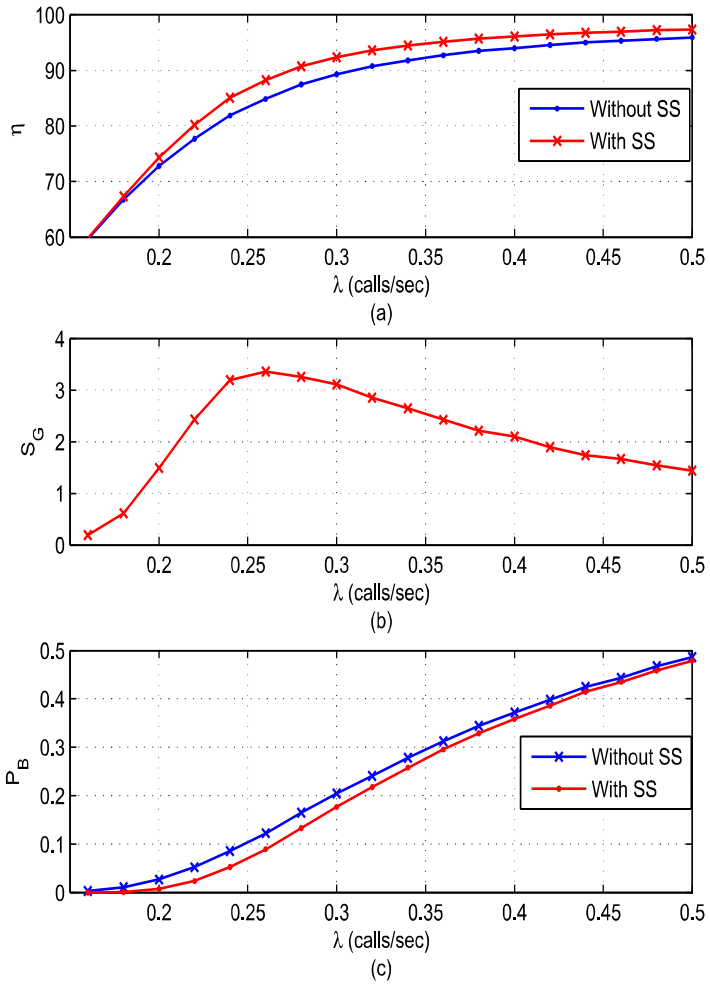

Figure 3.1: Comparison plots of (a) Spectrum efficiency vs λ (b) Spectrum efficiency gain vs λ and (c) Call blocking probability vs λ for the sharing and non-sharing case for same call arrival rate.

The three performance parameters mentioned above (η, S_G, P_B) are obtained by varying call arrival rate from 0.16 to 0.5 calls/sec. But while varying, it will be same for both the base stations i. e. BS1 and BS2.

From Fig. 3.1 (a), we can observe that the spectrum efficiency is same for without and with spectrum sharing for small values of $\lambda \leq 0.18$ calls/sec. This is because the users are getting served by own operator at lower call arrival rate. As call arrival rate, λ, increases, it yields more spectrum efficiency with sharing compared to without sharing. As a result in Fig. 3.1 (b), we can observe around 3.4% spectrum efficiency gain at 0.26 calls/sec arrival rate due to spectrum sharing. But, as λ increases above 0.26 calls/sec, gain starts decreasing due to lack of free resources in both the BSs. Fig. 3.1 (c) shows that call blocking probability reduces due to spectrum sharing. In practical scenario, call blocking probability, P_B, will be maintained strictly less than 0.1. A call arrival rate of 0.25 calls/sec gives $P_B = 0.1$ in the case without sharing. But, same blocking probability can be achieved at call arrival rate equal to 0.27 calls/sec by sharing spectrum when call arrival rates are same. So, by maintaining $P_B = 0.1$, BSs can serve 72 users/hour more in shared spectrum case.

case II : Call arrival rate λ_1 for BS1 is varying and for BS2, λ_2 is kept constant.

In this case, BS2 is kept at constant call arrival rate, λ_2 equal to 0.02 calls/sec which gives spectrum efficiency of 7.5% for BS2 without sharing. From Fig. 3.2, by varying call arrival rate, λ_1, for BS1, we can observe spectrum efficiency remains almost same for BS1 but it increases for BS2 with spectrum sharing.

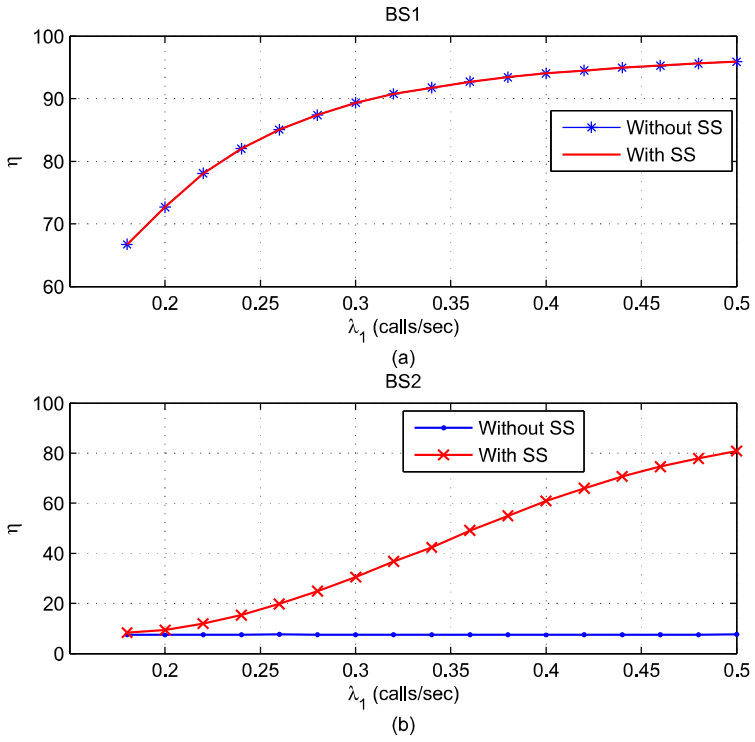

Figure 3.2: Comparison plots of (a) Spectrum Efficiency vs λ_1 for BS1 and (b) Spectrum efficiency vs λ_1 for BS2 with and without sharing case when λ_2 is constant.

This is result of calls are getting accommodated on BS2 due to lack of resources in BS1. Fig. 3.2 (b) shows the increment of spectrum utilization from 7.5% to 80% in BS2 at $\lambda = 0.5$ calls/sec.

Fig. 3.3 gives us the averaged spectrum efficiency gain over the spectrum occupied by both the

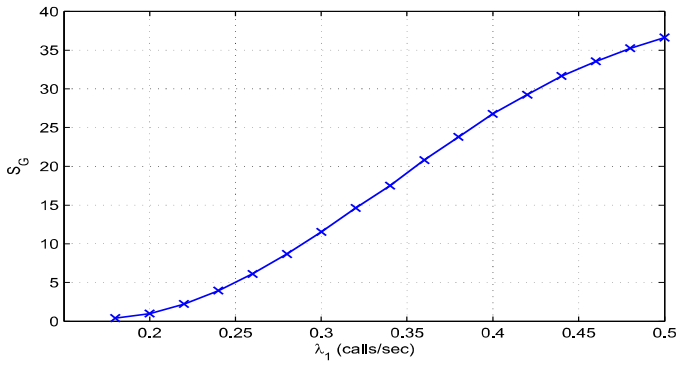

Figure 3.3: Spectrum Efficiency Gain vs λ_1 for constant λ_2.

base stations plotted against call arrival rate λ_1. The maximum spectrum efficiency gain of 38% is observed at the highest call arrival rate of 0.5 calls/sec in BS1.

The call blocking probability for BS1 reduces tremendously as calls are transferred to BS2 as shown in Fig. 3.4 (a). As shown in Fig. 3.4 (b), call blocking increases in BS2 at higher values of λ_1. Because, BS1 is utilizing the resources of BS2 and BS2 fails to serve his own users.

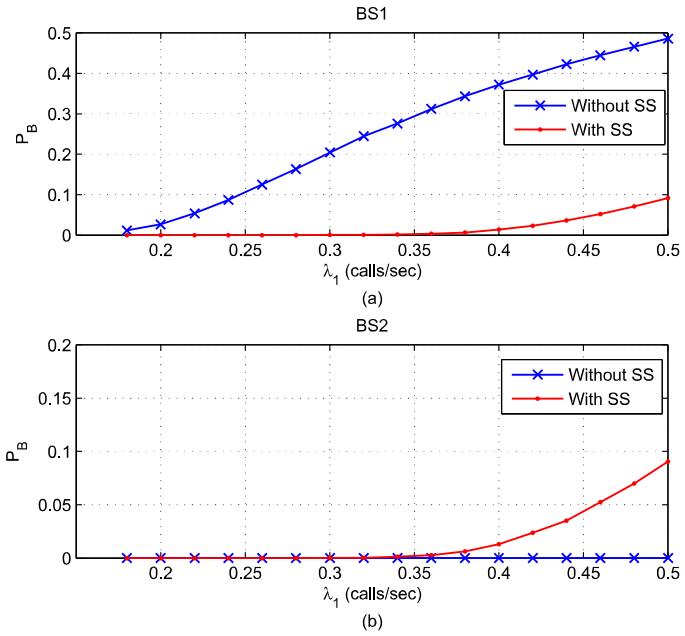

Figure 3.4: Comparison plots of (a) Call blocking probability vs λ_1 for BS1 and (b) Call blocking probability vs λ_1 for BS2 with and without sharing case keeping constant λ_2.

Fig. 3.4 (a) shows $P_B = 0.1$ at $\lambda_1 = 0.25$ calls/sec without sharing in BS1 and same blocking probability is obtained at $\lambda_1 = 0.5$ calls/sec by sharing. So, it concludes that BS1 with sharing can support traffic with double call arrival rate compared the one without sharing by keeping blocking probability below 0.1. BS1 can serve 900 users/hour more by keeping P_B below 0.1 when BS2 have less traffic load.

case III : Call arrival rates for the both BSs are different and both are varying.

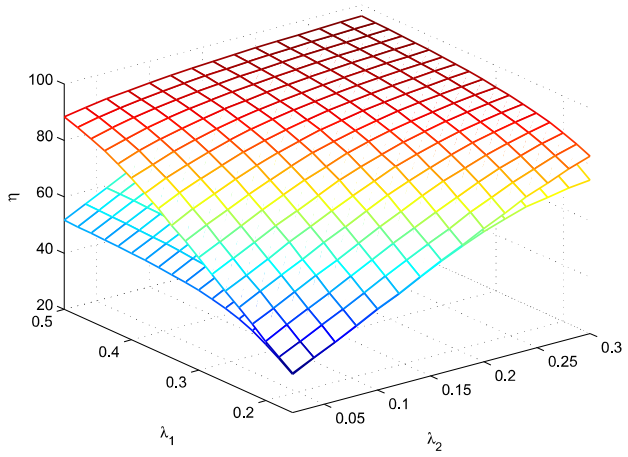

Figure 3.5: Spectrum efficiency vs λ_1 vs λ_2.

This is the most general case. Now, by independently varying call arrival rates i.e. λ_1, λ_2, we get 3-D plot of spectrum efficiency vs λ_1 vs λ_2 as shown in Fig. 3.5. The spectrum efficiency gain reduces as call arrival rates for BSs goes above 0.26 calls/sec as observed in case I. So, we are varying λ_1 from 0.16 calls/sec to 0.5 calls/sec and λ_2 from 0.02 calls/sec to 0.3 calls/sec. As the call arrival rates i.e λ_1 and λ_2 starts decreasing, then spectrum utilization with spectrum sharing reduces and finally drop down to spectrum utilization in case of without sharing.

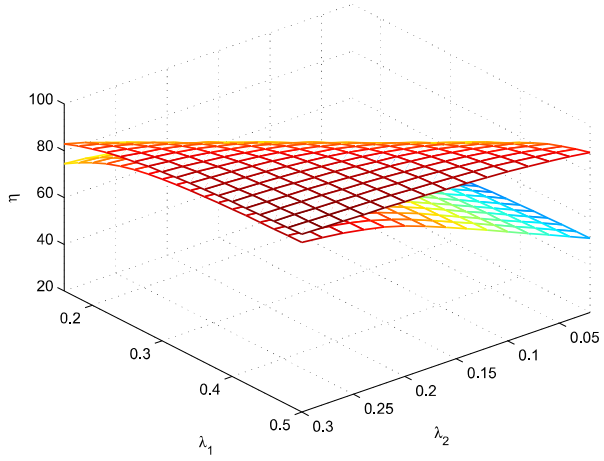

Figure 3.6: Another view of Spectrum efficiency vs λ_1 vs λ_2.

Fig. 3.6 gives the another view of 3-D plot shown in Fig. 3.5. In this view, we can easily observe that if both λ_1 and λ_2 increases, then spectrum utilization gap between cases with and without sharing reduces due to less free resources with both BSs at any particular time instant.

The spectrum efficiency gain 3-D plot is given in Fig. 3.7. From this figure, we can observe the maximum spectrum efficiency gain of 38% at $\lambda_1 = 0.5$ calls/sec and $\lambda_2 = 0.02$ calls/sec which we also observed in case II. The spectrum efficiency gain reduces as call arrival rate, λ_1, for BS1 decreases and call arrival rate, λ_2, for BS2 increases. The gain reduces to zero in two cases, first when both call arrival rates are very low and second when call arrival rates are very high. The spectrum sharing in these two cases is not useful.

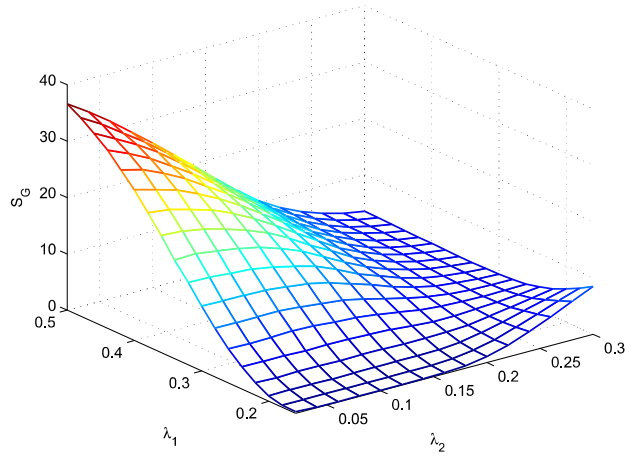

Figure 3.7: Spectrum efficiency gain vs λ_1 vs λ_2.

Fig. 3.8 gives the call blocking probability as a function of call arrival rates, λ_1 and λ_2. We can say that spectrum sharing reduces the chance of call getting blocked. When traffic load in both base stations is very high, then the blocking probability with spectrum sharing equals to the case without sharing. In other case, when call arrival rates are very low in both the BSs, P_B reduces to zero.

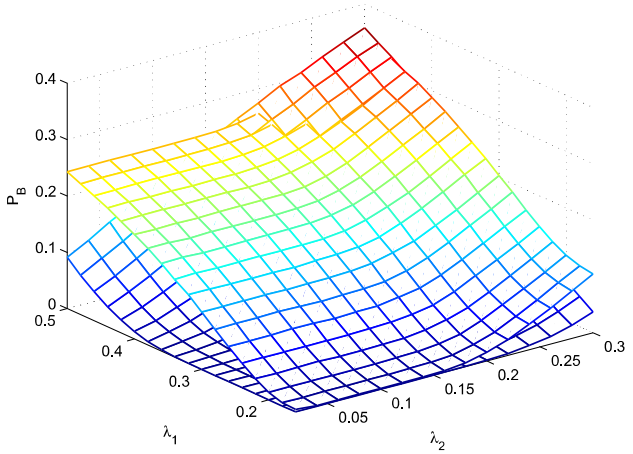

Figure 3.8: Call blocking probability vs λ_1 vs λ_2.

3.2.1 Region of Co-ordination (ROC)

ROC is a portion of graph with λ_1 as x-axis and λ_2 as y-axis having specific range of spectrum efficiency gain. For example, if we need gain greater than 1%, then ROC will be an area excluding lower-left corner having gain below 1%. Fig. 3.9 gives three regions with spectrum efficiency gain less than 1%, between 1 to 10% and greater than 10%. The dotted line represents that both BSs ara having same call arrival rate and point on dotted line is where we get maximum spectrum efficiency gain of 3.4% in same call arrival rate case.

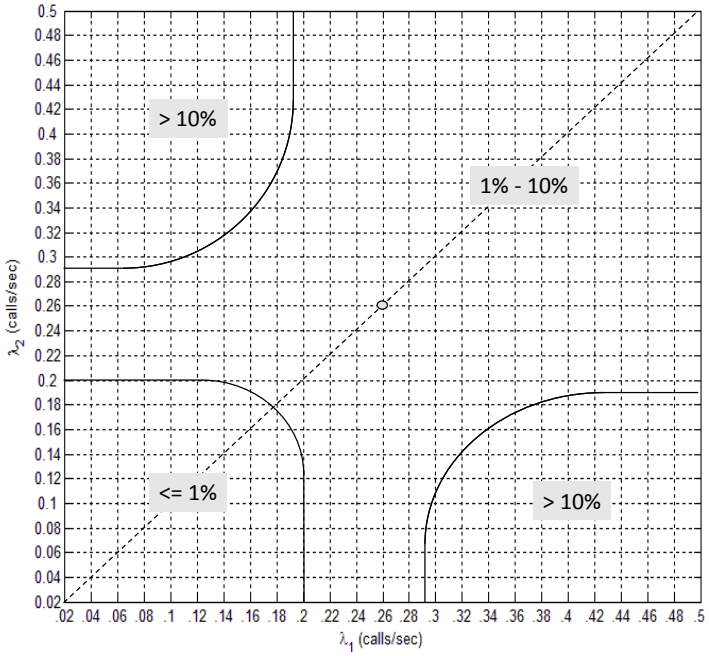

Figure 3.9: Region of Co-ordination showing different spectrum efficiency gains for two GSM operators.

3.3 3-BS

The performance parameters will be evaluated again by allowing the spectrum sharing between three GSM operators with co-located base stations.

case I : Call arrival rates are same for all the three BSs i.e. $\lambda_1 = \lambda_2 = \lambda_3$.

The same call arrival rate is varied from 0.18 calls/sec to 0.5 calls/sec and we get spectrum efficiency (η), gain achieved (S_G) and call blocking probability (P_B) as shown in Fig. 3.10. The spectrum utilization/efficiency with spectrum sharing starts increasing compared to without sharing for $\lambda \geq 0.18$ calls/sec as shown in Fig. 3.10 (a). From Fig. 3.10 (b), we can observe maximum spectrum efficiency gain, S_G, of 4.95% at call arrival rate of 0.26 calls/sec. After this point, gain again starts decreasing due to the lack of free resources in BSs.

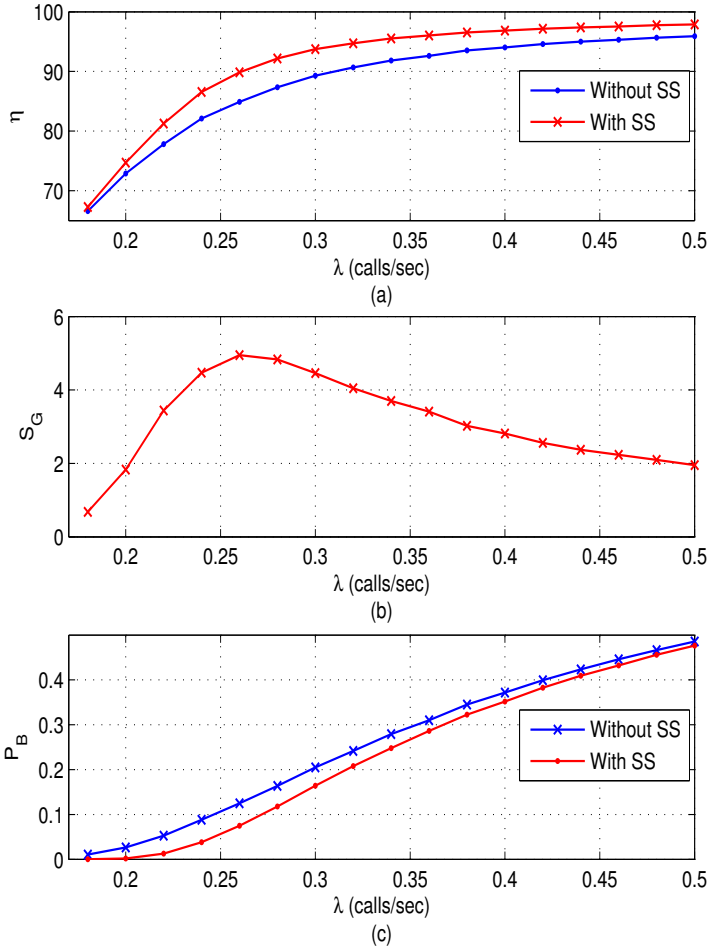

Figure 3.10: Comparison plots of (a) Spectrum efficiency vs λ (b) Spectrum efficiency gain vs λ and (c) Call blocking probability vs λ for the sharing and non-sharing case for same call arrival rate.

From Fig. 3.10 (c), we can see that the call blocking probability, P_B, is equal to 0.1 at $\lambda = 0.25$ calls/sec in the case of without sharing. In sharing case, same call blocking probability of 0.1 can

be observed at $\lambda = 0.275$ calls/sec. BSs can serve 90 users/hour more due to spectrum sharing by maintaining blocking probability of 0.1 in case of same call arrival rate for all the three BSs.

case II : Call rate λ_1 for BS1 is varying and λ_2 for BS2, λ_3 for BS3 are kept constant.

In case of three base stations, the best case (with highest efficiency gain) is the one when one of base stations is having high traffic and other two with very low traffic. So, call arrival rates, λ_1 and λ_2 are kept constant at 0.02 calls/sec. The spectrum efficiency in BS1 remains same as it is highly loaded with traffic as shown in Fig. 3.11 (a).

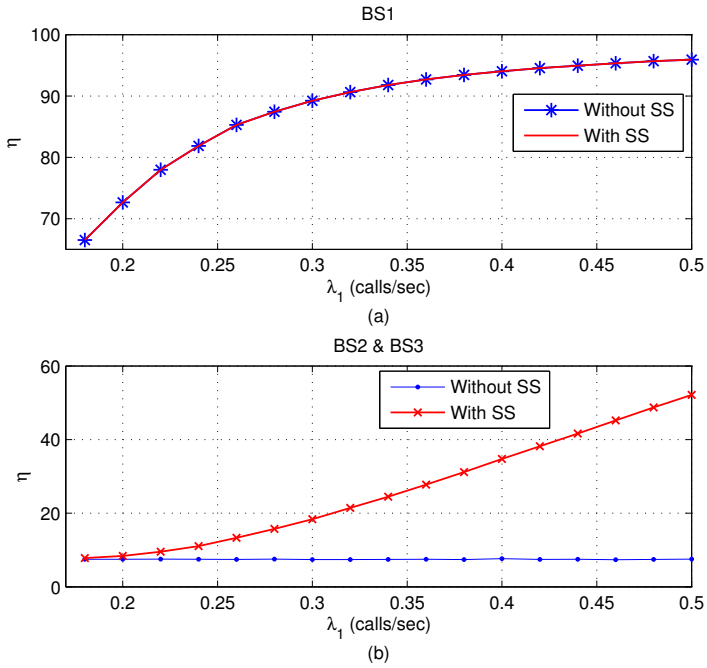

Figure 3.11: Comparison plots of (a) Spectrum Efficiency vs λ_1 for BS1 and (b) Spectrum efficiency vs λ_1 for BS2 and BS3 with and without sharing case when λ_2 is constant.

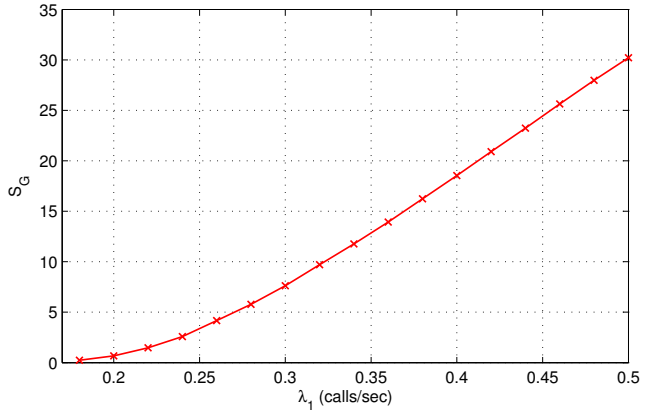

Figure 3.12: spectrum efficiency gain vs λ_1 for constant λ_2.

BS1 just transfers extra traffic to other two BSs and it gets equally distributed among BS2 and BS3. So, spectrum utilization with and without spectrum sharing is same for both the BSs (BS2 and BS3) as shown in Fig. 3.11 (b). Fig. 3.12 shows maximum spectrum efficiency gain of 30% at $\lambda_1 = 0.5$ calls/sec as result of an increment in spectrum efficiency of two BSs.

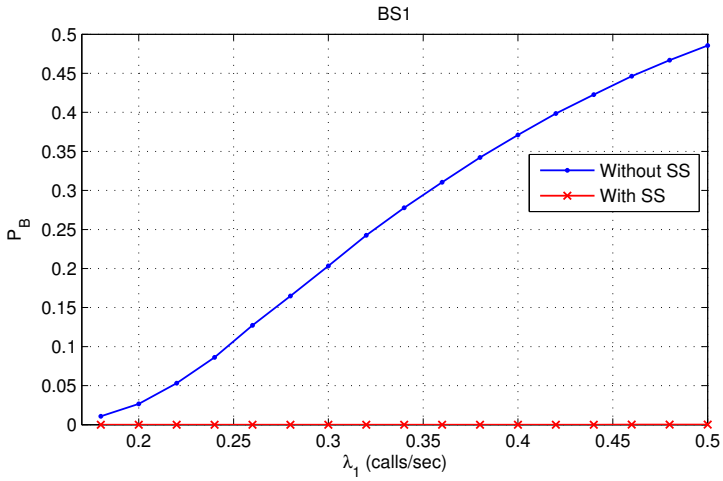

Figure 3.13: Call blocking probability vs λ_1 for BS1 with and without sharing case keeping constant λ_2.

The whole extra traffic from BS1 gets served by BS2 and BS3 without any call drop. So, from Fig. 3.13, we can observe that call blocking probability comes down to zero. Without sharing, call blocking probability, P_B, is equal to 0.1 at $\lambda_1 = 0.25$ calls/sec for BS1. With sharing, BS1 can serve traffic with double call arrival rate and zero call blocking probability.

3.4 Comparison between 2-BS and 3-BS

case I: call arrival rates for all base stations in co-ordination are same.

From Fig. 3.14, we can observe maximum increment of 1.55% gain in case of 3-BS compared to 2-BS at call arrival rate of 0.26 calls/sec. This is because one operator users are utilizing free resources of two other operators rather than one. The gap between these two cases reduces after call arrival rate of 0.26 calls/sec.

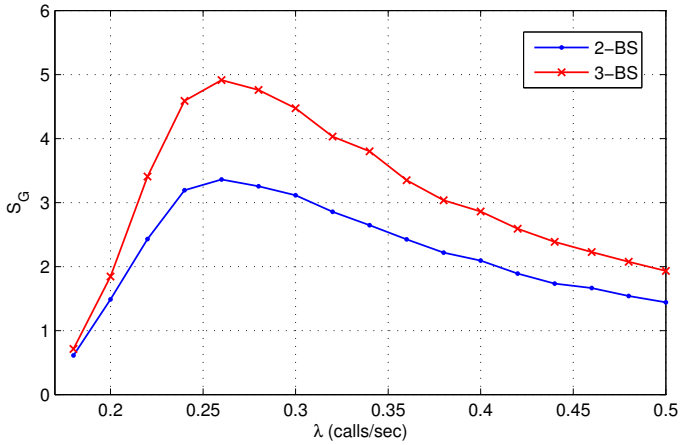

Figure 3.14: spectrum efficiency, spectrum efficiency gain and blocking probability vs call arrival rate λ in three base station case.

case II: call arrival rate, λ_1, for BS1 is varying and low call arrival rate of 0.02 calls/sec for other BSs in co-ordination.

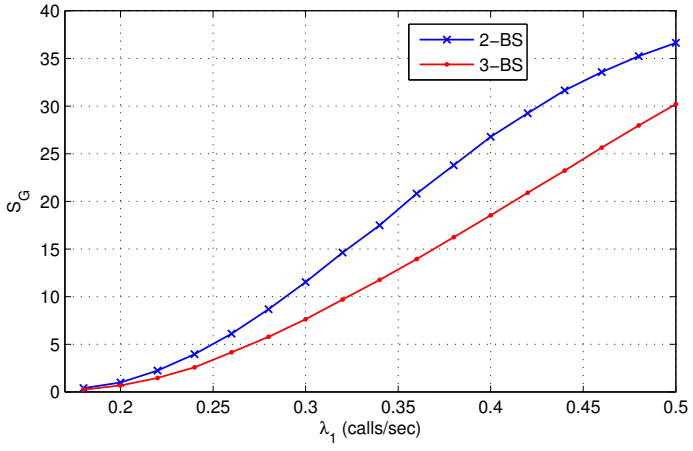

Figure 3.15: spectrum efficiency, spectrum efficiency gain and blocking probability vs call arrival rate λ in three base station case.

In both the cases, maximum efficiency gain is achieved at $\lambda_1 = 0.5$ calls/sec as shown in Fig.

3.15. The maximum gain in 3-BS is less compared to 2-BS. The reason is that spectrum efficiency gain is averaged over the gains in each BS.

3.4.1 Practical Feasibility

CSC in system architecture is a piece of code and not an independent physical entity. So, there is no need of extra hardware. CSC takes decision when co-ordination is needed based on ROC. It also perform steps for carrier sharing as mentioned in flowchart in Fig. 2.2. Due to sharing, one operator's users are using other operator resources. So, for this, settlement should be done between two GSM operators. This issue should be considered in GSM pricing.

Chapter 4

Low Complexity Spectrum Sensing Algorithm Robust to Noise Uncertainty

Robust spectrum sensing is a fundamental component in cognitive radio due to the noise uncertainty. In this chapter, we propose a robust spectrum sensing algorithm based on the covariance matrix of signals received at the secondary users. The proposed method can even perform better than the ideal energy detection even if the received signals are highly correlated. The test statistic used in the algorithm is dependent on mean and standard deviation of eigenvalues and can be calculated from the trace of covariance matrix and trace of square of the covariance matrix. Simulations verifying the robustness and performance of the proposed algorithm are presented.

4.1 Introduction

Cognitive Radio uses spectrum sensing to determine unoccupied frequency bands [22, 23, 24]. This gives rise to an opportunistic spectrum access for secondary users in an unused radio spectrum by primary licensed users.

Spectrum sensing plays very important role in a cognitive radio. But it is challenging due to low received primary signal SNR, multipath fading and noise uncertainty [25, 26, 27].

Many spectrum sensing techniques, each with its own prerequisites, such as the energy detection [25, 26, 27, 28, 29], matched filtering [30, 31, 25, 32, 33, 29] and cyclostationary detection [34, 35, 36, 37] have been developed. Cyclostationary detection needs the knowledge of cyclic frequencies of the primary user signal and matched filtering requires an information about channel and waveforms of primary user. Compared to these techniques, energy detection does not need any information of the signal but needs the knowledge of exact noise power. Inaccuracy in the calculation of the noise power results into high probability of false alarm [26, 27, 38]. Also, energy detection performs better for detecting independent and identically distributed (iid) signal [29]. But in case of the detection of correlated signal, there is degradation in the performance of energy detection. The noise uncertainty is an outcome of non-linearity of receiver components and transmissions of other users. The proposed algorithm overcomes the noise uncertainty and correlation problem of energy detection.

Test statistic based on the covariance matrix of the received signal is proposed. The proposed method performs much better compared to the energy detection. The test statistic used in the proposed algorithm is obtained by using an MMSE (minimum mean square estimation) to obtain an approximation to the average to minimum eigenvalue ratio of covariance matrix.

The rest of the chapter is organized as follows. In Section 4.2, the system model is presented. The new algorithm for spectrum sensing is proposed in the Section III. Section IV gives derivation of the proposed algorithm and analyzes the computational complexity involved in the algorithm. Simulation results are provided in the Section V and conclusions in Section VI.

4.2 System Model

Let $x_c(t) = s_c(t) + \eta_c(t)$ be the continuous-time received signal with primary user's signal $s_c(t)$ and the noise $\eta_c(t)$ is zero mean i.e. $E(\eta_c(t)) = 0$ and variance $E(\eta_c^2(t)) = \sigma_\eta^2$. Let the frequency band over which sensing is performed be W. We select a sampling rate f_s for the received signal that should be greater than or equal to W based on the Nyquist criteria. Take $T_s = 1/f_s$ as the sampling interval. Using this sampling interval, we define discrete time signals as $x(n) \doteq x(nT_s)$, $\overline{s}(n) \doteq s_c(nT_s)$ and $\eta(n) \doteq \eta_c(nT_s)$. There are two hypothesizes: (1) H_0: only noise is present; (2) H_1: both signal and noise is present. The received signal under the two hypothesizes, is given by [25]−[33]

$$H_0 : x(n) = \eta(n), \tag{4.1}$$

$$H_1 : x(n) = \overline{s}(n) + \eta(n) \tag{4.2}$$

where $\overline{s}$(n) is the received signal samples which includes the effect of multipath fading and $\eta(n)$ is received white noise assumed to be independent and identically distributed(iid).

Let $s(n)$ be the digital source signal with the symbol duration as T_0. The discrete signal is transmitted through the communication channel and the resultant signal, including channel response $h(t)$, but excluding the noise, is given as

$$s_c(t) = \sum_{k=-\infty}^{\infty} s(k)h(t - kT_0), \tag{4.3}$$

Suppose that the received signal is over-sampled by a factor M, i.e. $T_s = T_0/M$. Define

$$\begin{aligned} x_i(n) &= x((nM + i - 1)T_s), \\ h_i(n) &= h((nM + i - 1)T_s), \\ \eta_i(n) &= \eta_c((nM + i - 1)T_s), \\ \text{where} &\quad n = 0, 1, \cdots \text{ and } i = 1, 2, \cdots, M. \end{aligned} \tag{4.4}$$

Considering multiple source signals (multiple transmit antennas), the received signal is given by

$$x_i(n) = \sum_{j=1}^{P} \sum_{k=0}^{N_{ij}} h_{ij}(k)s_j(n - k) + \eta_i(n), \tag{4.5}$$

where P is the number of source signals, $h_{ij}(k)$ is the channel response from source signal j, and N_{ij} is the order of channel.

The proposed algorithm is based on the statistical covariance matrix [39]. Let $N_j \stackrel{def}{=} \max_i(N_{ij})$, zero-padding $h_{ij}(k)$; if needed, and defining

$$\mathbf{x}(n) \stackrel{def}{=} [x_1(n), x_2(n), \cdots, x_M(n)]^T, \tag{4.6}$$

$$\mathbf{h}_j(n) \stackrel{def}{=} [h_{1j}(n), h_{2j}(n), \cdots, h_{Mj}(n)]^T, \tag{4.7}$$

$$\boldsymbol{\eta}(n) \stackrel{def}{=} [\eta_1(n), \eta_2(n), \cdots, \eta_M(n)]^T. \tag{4.8}$$

Using (4.6), (4.7) and (4.8), (4.5) can be written in vector form as

$$\mathbf{x}(n) = \sum_{j=1}^{P} \sum_{k=0}^{N_j} \mathbf{h}_j(k)s_j(n - k) + \boldsymbol{\eta}(n), n = 0, 1, \cdots. \tag{4.9}$$

By averaging over "L" consecutive symbols, define

$$\begin{aligned} \hat{\mathbf{x}}(n) &\stackrel{def}{=} [\mathbf{x}^T(n), \mathbf{x}^T(n-1), \cdots, \mathbf{x}^T(n - L + 1)]^T, \\ \hat{\boldsymbol{\eta}}(n) &\stackrel{def}{=} [\boldsymbol{\eta}^T(n), \boldsymbol{\eta}^T(n-1), \cdots, \boldsymbol{\eta}^T(n - L + 1)]^T, \\ \hat{\mathbf{s}}(n) &\stackrel{def}{=} [s_1(n), s_1(n-1), \cdots, s_1(n - N_1 - L + 1), \cdots, \\ &\qquad s_p(n), s_p(n-1), \cdots, s_p(n - N_p - L + 1)]^T \end{aligned} \tag{4.10}$$

Using (4.9) in $\hat{\mathbf{x}}(n)$ and then substituting in (4.10), we have

$$\hat{\mathbf{x}}(n) = H\hat{\mathbf{s}}(n) + \hat{\boldsymbol{\eta}}(n) \tag{4.11}$$

where H is a ML×(N+PL)($N \stackrel{def}{=} N_1 + \cdots + N_p$) matrix defined as

$$H \stackrel{def}{=} [H_1, H_2, \cdots, H_p] \tag{4.12}$$

$$H_j \stackrel{def}{=} \begin{bmatrix} \mathbf{h}_j(0) & \cdots & \cdots & \mathbf{h}_j(N_j) & \cdots & 0 \\ & \ddots & & & \ddots & \\ 0 & \cdots & \mathbf{h}_j(0) & \cdots & \cdots & \mathbf{h}_j(N_j) \end{bmatrix} \tag{4.13}$$

Note that the dimension of H_j is ML×(N_j+L).

Define statistical covariance matrices of the signals and noise as

$$\mathbf{R}_x = E(\hat{\mathbf{x}}(n)\hat{\mathbf{x}}^\dagger(n)), \tag{4.14}$$

$$\mathbf{R}_s = E(\hat{\mathbf{s}}(n)\hat{\mathbf{s}}^\dagger(n)), \tag{4.15}$$

$$\mathbf{R}_\eta = E(\hat{\boldsymbol{\eta}}(n)\hat{\boldsymbol{\eta}}^\dagger(n)). \tag{4.16}$$

Then, we get

$$\mathbf{R}_x = H\mathbf{R}_s H^\dagger + \sigma_\eta^2 \mathbf{I}_{ML}, \tag{4.17}$$

where σ_η^2 is the variance of the noise and $\mathbf{I}_{ML}$ is the identity matrix of order ML.

4.3 The Proposed Algorithm

In this section we present the proposed algorithm, which is as follows:

Step 1. Compute the sample covariance matrix of the received signal.

$$\mathbf{R}_x(N_s) \stackrel{def}{=} \frac{1}{N_s} \sum_{n=L-1}^{L-2+N_s} \hat{\mathbf{x}}(n)\hat{\mathbf{x}}^\dagger(n),$$

where N_s is the number of collected samples.

Step 2. Obtain the test statistic of the matrix $\mathbf{A} = \mathbf{R}_x(N_s)$ as follows

$$\hat{C}_E = a_0 + a_1 C_{EL} + a_2 C_{EU}$$

where,

$$C_{EL} = \frac{m}{m - s/(n-1)^{1/2}}$$

$$C_{EU} = \begin{cases} \frac{m}{m - s(n-1)^{1/2}} & \lambda_{minl} \neq 0 \\ \infty & \lambda_{minl} = 0 \end{cases}$$

$$m = \frac{trace(\mathbf{A})}{n}, s^2 = \frac{trace(\mathbf{A}^2) - (trace(\mathbf{A}))^2/n}{n},$$

$n = ML$ and a_0, a_1, a_2 are constants.(The design of these constants is considered in Section 4.4.)

Step 3. Decision: if $\hat{C}_E > \gamma$, signal exists: otherwise, signal does not exist. The threshold, $\gamma > 1$, is chosen; as given in the Appendix.

4.4 Derivation of the algorithm

In subsection 4.4.1, we review the results on the upper and lower bounds of minimum eigenvalue as given in [40]. In subsection 4.4.2, we use the upper and lower bounds on the minimum eigenvalue to derive an MMSE approximation to the energy with minimum eigenvalue ratio.

4.4.1 Upper and Lower bounds on the Test Statistic

Suppose $\mathbf{A}$ be an n×n square matrix, then eigenvalues of $\mathbf{A}$, are the roots of the characteristic equation given by

$$det(\mathbf{A} - \lambda I) = 0.$$

The standard deviation of the eigenvalues, denoted by s, is given by [40]

$$\begin{aligned} s^2 &= \frac{1}{n}\left(\sum_{j=1}^{n}\lambda_j^2 - \frac{1}{n}\left(\sum_{j=1}^{n}\lambda_j\right)^2\right) \\ &= \frac{trace(\mathbf{A}^2) - (trace(\mathbf{A}))^2/n}{n}. \end{aligned} \tag{4.18}$$

The mean of the eigenvalues in the terms of trace of the matrix, $\mathbf{A}$, is given by [40]

$$m = \frac{1}{n}\left(\sum_{j=1}^{n}\lambda_j\right) = \frac{trace(\mathbf{A})}{n}. \tag{4.19}$$

We know that the eigenvalues are real if and only if $\mathbf{A}$ is Hermitian; which is true for any covariance matrix. The bounds on the minimum eigenvalue are dependent on the mean, m, and the standard deviation, s, of eigenvalues.

Lemma 1. *(Theorem 2.1, [40]) Let* $\mathbf{A}$ *be an n×n complex matrix with real eigenvalues* $\lambda(\mathbf{A})$ *and consider* m *and* s^2 *defined previously. Then*

$$m - s(n-1)^{1/2} \leq \lambda_{min}(\mathbf{A}) \leq \underbrace{m - s/(n-1)^{1/2}}_{\lambda_{minu}} \tag{4.20}$$

But, as we know that the eigenvalues of covariance matrix are always positive. So, lower bound on minimum eigenvalue can be rewritten as $\lambda_{minl} = max(0, m - s(n-1)^{1/2})$.

Now, the energy to minimum eigenvalue ratio is defind as

$$C_E = \frac{T(N_s)}{\lambda_{min}} \tag{4.21}$$

where $T(N_s)$ is the average power of received signal as given below.

$$T(N_s) = \frac{1}{MN_s}\sum_{i=1}^{M}\sum_{n=0}^{N_s-1}|x_i(n)|^2, \tag{4.22}$$

Using the fact that the average received signal power, $T(N_s)$, is equal to the average of eigevalues, m, as derived in Appendix and using bounds on λ_{min}, we get the upper and lower bounds on the

test statistic as follows:

$$C_{EL} = \frac{m}{m - s/(n-1)^{1/2}} \tag{4.23}$$

$$C_{EU} = \begin{cases} \frac{m}{m - s(n-1)^{1/2}} & \lambda_{minl} \neq 0 \\ \infty & \lambda_{minl} = 0 \end{cases} \tag{4.24}$$

The lower bound on the energy to minimum eigevalue ratio, C_{EL}, given in (4.23), and the upper bound, C_{EU}, given in (4.24), are used to obtain the test statistic in next subsection. But, when $\lambda_{minl} = 0$, then C_{EU} goes to infinity. In that case, we will use just lower bound, C_{EL}, for deriving the test statistic.

4.4.2 Test Statistic using MMSE

The test statistic, $\hat{C}_E$, is obtained using lower bound, C_{EL}, and upper bound, C_{EU} so that MSE is minimized. We have

Theorem 1. *Let the test statistic, $\hat{C}_E$ be the estimated value of the energy to minimum eigenvalue given by*

$$\hat{C}_E = a_0 + a_1 C_{EL} + a_2 C_{EU}. \tag{4.25}$$

Then MSE(mean squared error) is minimized if

$$a_1 = \begin{cases} \frac{\sigma_{CL}}{\sigma_L^2}, & C_{EU} = \infty \\ \frac{\sigma_U^2 \sigma_{CL} - \sigma_{LU}\sigma_{CU}}{\sigma_L^2 \sigma_U^2 - (\sigma_{LU})^2}, & C_{EU} \neq \infty \end{cases} \tag{4.26}$$

$$a_2 = \begin{cases} 0 & C_{EU} = \infty \\ \frac{\sigma_L^2 \sigma_{CU} - \sigma_{LU}\sigma_{CL}}{\sigma_L^2 \sigma_U^2 - (\sigma_{LU})^2}, & C_{EU} \neq \infty \end{cases} \tag{4.27}$$

$$a_0 = \begin{cases} \mu_C - a_1 \mu_L, & C_{EU} = \infty \\ \mu_C - a_1 \mu_L - a_2 \mu_U. & C_{EU} \neq \infty \end{cases} \tag{4.28}$$

Proof. Case 1: $C_{EU} = \infty$
Here, $\hat{C}_E$ is given by

$$\hat{C}_E = a_0 + a_1 C_{EL} \tag{4.29}$$

The mean squared error in this case defined as follows.

$$E[(C_E - \hat{C}_E)^2] = E[(C_E - a_0 - a_1 C_{EL})^2]. \tag{4.30}$$

To minimize MSE, differentiate it with respect to a_0, a_1, then equate derivatives to zero. Differentiating (4.30) with respect to a_0 by taking derivative inside expectation and equating to zero, we get

$$E[(C_E - a_0 - a_1 C_{EL})(-2)] = 0,$$

Simplifying for a_0, we get

$$a_0 = E[C_E] - a_1 E[C_{EL}].$$

Defining $E[C_E] = \mu_C$, $E[C_{EL}] = \mu_L$, we get

$$a_0 = \mu_C - a_1\mu_L. \tag{4.31}$$

Substituting this value of a_0 into (4.25), we get

$$\hat{C}_E = \mu_C + a_1(C_{EL} - \mu_L).$$

Rewrite MSE as follows

$$E[((C_E - \mu_C) - (\hat{C}_E - \mu_C))^2] = E[(\overline{C}_E - a_1\overline{C}_{EL})^2], \tag{4.32}$$

where, $\overline{C}_E = C_E - \mu_C$, $\overline{C}_{EL} = C_{EL} - \mu_L$. Differentiating (4.32) with respect to a_1, we get

$$E[(\overline{C}_E - a_1\overline{C}_{EL})\overline{C}_{EL}] = 0, \tag{4.33}$$

Define the covariance terms $E[C_E C_{EL}] = \sigma_{CL}$, $E[C_{EL}C_{EL}] = \sigma_L^2$ substituting this into (4.33), we get

$$a_1 = \frac{\sigma_{CL}}{\sigma_L^2}. \tag{4.34}$$

Finally putting this value of a_1 into (4.31), we get value of a_0.

Case 2: $E_U \neq \infty$

The mean squared error is defined as

$$E[(C_E - \hat{C}_E)^2] = E[(C_E - a_0 - a_1C_{EL} - a_2C_{EU})^2]. \tag{4.35}$$

To minimize MSE, we differentiate it with respect to a_0, a_1 and a_2, then set each of the derivatives to zero. Differentiating (4.35) with respect to a_0 and taking derivative inside the expectation, we get

$$E[(C_E - a_0 - a_1C_{EL} - a_2C_{EU})(-2)] = 0.$$

Taking a_0 terms on left hand side and rest on right hand side and simplifying, we have

$$a_0 = E[C_E] - a_1E[C_{EL}] - a_2E[C_{EU}].$$

Defining $E[C_E] = \mu_C$, $E[C_{EL}] = \mu_L$ and $E[C_{EU}] = \mu_U$, we get

$$a_0 = \mu_C - a_1\mu_L - a_2\mu_U. \tag{4.36}$$

Putting this value of a_0 into equation (4.25), we obtain

$$\hat{C}_E = \mu_Y + a_1(C_{EL} - \mu_L) + a_2(C_{EU} - \mu_U)$$

Rewrite mean square error criterion as

$$E[((C_E - \mu_C) - (\hat{C}_E - \mu_C))^2] = E[(\overline{C}_E - a_1\overline{C}_{EL} - a_2\overline{C}_{EU})^2] \tag{4.37}$$

where,

$\overline{C}_E = C_E - \mu_C$, $\overline{C}_{EL} = C_{EL} - \mu_L$, $\overline{C}_{EU} = C_{EU} - \mu_U$. Differentiating (4.37) with respect to a_1, we get

$$E[(\overline{C}_E - a_1\overline{C}_{EL} - a_2\overline{C}_{EU})\overline{C}_{EL}] = 0. \tag{4.38}$$

Define the covariance terms

$$\begin{aligned}
&E[\overline{C}_E\overline{C}_{EL}] = \sigma_{CL}, E[\overline{C}_E\overline{C}_{EU}] = \sigma_{CU},\\
&E[\overline{C}_{EL}\overline{C}_{EU}] = \sigma_{LU}, E[\overline{C}_{EL}\overline{C}_{EL}] = \sigma_L^2,\\
&E[\overline{C}_{EU}\overline{C}_{EU}] = \sigma_U^2.
\end{aligned}$$

Substituting these terms in (4.38), we obtain

$$a_1\sigma_L^2 + a_2\sigma_{LU} = \sigma_{CL}. \tag{4.39}$$

Similarly, differentiating (4.37) with respect to a_2, we get

$$a_1\sigma_{LU} + a_2\sigma_U^2 = \sigma_{CU}. \tag{4.40}$$

Collecting the (4.39) and (4.40) in the matrix form, we get

$$\begin{bmatrix} \sigma_L^2 & \sigma_{LU} \\ \sigma_{LU} & \sigma_U^2 \end{bmatrix} \begin{bmatrix} a_1 \\ a_2 \end{bmatrix} = \begin{bmatrix} \sigma_{CL} \\ \sigma_{CU} \end{bmatrix}. \tag{4.41}$$

Solving for constants a_1 and a_2, we get

$$\begin{bmatrix} a_1 \\ a_2 \end{bmatrix} = \begin{bmatrix} \sigma_L^2 & \sigma_{LU} \\ \sigma_{LU} & \sigma_U^2 \end{bmatrix}^{-1} \begin{bmatrix} \sigma_{CL} \\ \sigma_{CU} \end{bmatrix}.$$

Taking inverse of 2×2 matrix, we have

$$\begin{bmatrix} a_1 \\ a_2 \end{bmatrix} = \frac{1}{\sigma_L^2\sigma_U^2 - (\sigma_{LU})^2} \begin{bmatrix} \sigma_U^2 & -\sigma_{LU} \\ -\sigma_{LU} & \sigma_L^2 \end{bmatrix} \begin{bmatrix} \sigma_{CL} \\ \sigma_{CU} \end{bmatrix}.$$

Simplifying, we get

$$\begin{aligned}
a_1 &= \frac{\sigma_U^2\sigma_{CL} - \sigma_{LU}\sigma_{CU}}{\sigma_L^2\sigma_U^2 - (\sigma_{LU})^2}\\
a_2 &= \frac{\sigma_L^2\sigma_{CU} - \sigma_{LU}\sigma_{CL}}{\sigma_L^2\sigma_U^2 - (\sigma_{LU})^2}.
\end{aligned}$$

putting a_1 and a_2 values in equation (4.36), we get a_0. □

4.4.3 Implementation Issues

For the implementation of the algorithm, we need the values of a_0, a_1 and a_2 in advance and these values are dependent on μ_C, μ_L, μ_U and σ_L^2, σ_U^2, σ_{LU}, σ_{CL}, σ_{CU}. These values can be precomputed using numerical integration for a given distribution of the entries of $\mathbf{A}$.

Even if the distribution is unknown then also the values of a_0, a_1 and a_2 are obtained using initial training for N sequences. For example μ_L is obtained as

$$\mu_L = \frac{1}{N}\sum_{i=1}^{N} C_{ELi}. \tag{4.42}$$

Similarly, we can obtain the values of μ_U and μ_C. The value of σ_L^2 is evaluated as

$$\sigma_L^2 = \frac{1}{N}\sum_{i=1}^{N}(C_{ELi} - \mu_L)^2. \tag{4.43}$$

Similar equation can be used to obtain the value of σ_U^2. Finally, the value of σ_{LU} obtained as

$$\sigma_{LU} = \frac{1}{N}\sum_{i=1}^{N}(C_{ELi} - \mu_L)(C_{EUi} - \mu_U). \tag{4.44}$$

We can obtain the values of σ_{CL} and σ_{CU} using similar formula as for σ_{LU} (4.44).

In both the cases, the constants are precomputed, so it does not increase computational complexity in the actual implementation of the algorithm.

4.4.4 Computational Complexity

The complexity of EME comes from two parts: 1) computation of the covariance matrix. 2) the eigenvalue decomposition of the covariance matrix. In the first part, covariance matrix, after reception of every sample, we need ML multiplications and M^2L^2 additions. In the EME algorithm, for calculation of the EME Ratio after reception of $(L-2+N_s)$ samples, total complexity involved, in flops, is given by [39]

$$O(M^3L^3). \tag{4.45}$$

For the proposed algorithm, there again two parts. The computational complexity of the covariance is same. The complexity of computation for evaluating m is $ML-1$ additions and 1 multiplication. The complexity in evaluation of $trace(A^2)$ is M^2L multiplications and $ML-1$ additions as every row of covariance matrix contains M elements with high value compared to rest due to oversampling. So, calculation of s^2 requires M^2L+3 multiplications and M^2L additions. Given m, s^2, the lower and upper bound on the EME Ratio, C_{EL} and C_{EU}, needs 2 square roots (typically a square root is equivalent to a multiplication), (4) multiplications, 2 additions. Finally, 2 multiplications and 2 additions are needed to calculate the test statistic($\hat{C}_E$). The overall complexity of the proposed algorithm for calculating the test statistic after reception of $(L-2+N_s)$ samples (in flops) is

$$2\,L\,M^2 + L\,M + 15. \tag{4.46}$$

So, compared to the original EME algorithm, proposed algorithm has ML^2 times less computations.

4.5 Simulations

In this section, we present simulation results based on the randomly generated BPSK signals. We consider a 2-input 4-receiver system ($M = 4, P = 2$). The channel orders are $N_1 = N_2 = 9$ (10 taps). The channel taps are complex Gaussian distribution with zero mean and a unit variance. Results are averaged over 1000 Monte Carlo realizations.

Figure 4.1 gives the probability of detection for the proposed algorithm and EME detection with fixed $L = 8, N_s = 100000, P_f = 0.1$. Observing, we can say that there is no degradation in the performance of proposed algorithm compared to EME detection. Infact, the proposed algorithm performs better for some SNRs.

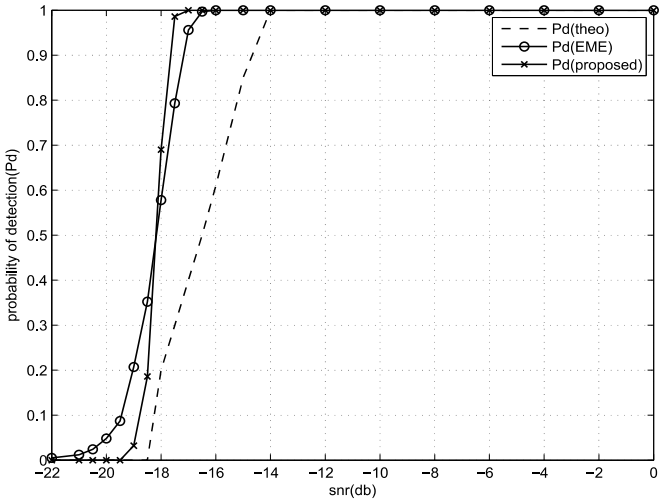

Figure 4.1: P_d vs SNR plots for the proposed algorithm, EME detection and the theoretical lower bound.

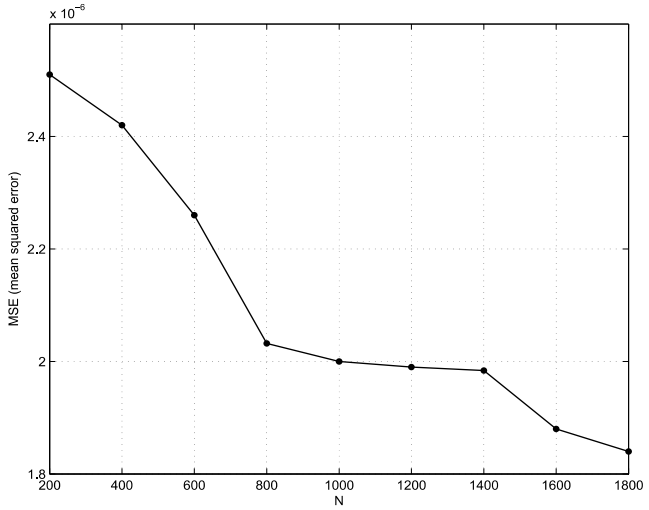

Figure 4.2: MSE (mean squared error) vs N.

The time required to calculate energy to minimum eigenvalue ratio using functions is 20 msec and test statistic takes only 0.11 msec (Results are obtained by running matlab programs on system with following configuration: Intel(R)Core(TM) i7-2600 CPU@3.40GHz, 4 Core(s)and 8GB RAM). Finally, also note that the theoretical lower bound given by (4.51) is within 1 db at very low SNRs but is loose as the SNR increases.

The change in the probability of detection of proposed algorithm compared to EME algorithm is due to the coloured noise depending on the snr values of received signal. The mean squared error (MSE) given by (4.35) in the calculation of test statistic using MMSE technique decreases as number of monte carlo realizations, N, increases as shown in Figure 4.2. We can also observe that mean squared error is getting saturated due to the coloured noise at higher values of N.

4.6 Conclusions

A spectrum sensing algorithm based on sample covariance matrix of the received signals has been proposed. The test statistic based on the lower bound of eigenvalues and trace of sample covariance matrix is obtained using MMSE technique. The computations involved in the calculation of test statistic is ML^2 times less as compared to EME algorithm. With reduced complexity, the proposed algorithm retains the robustness of EME algorithm as verified by simulation results.

4.7 Appendix

In this section, we show that as N_s tends to infinity, the test statistic tends to the energy to minimum eigenvalue ratio. This allows us to apply the theoretical analysis given in [39] to the proposed algorithm. In the absence of signal, $R_x(N_s)$ turns to the sample covariance matrix of noise, $R_\eta(N_s)$ given by

$$\mathbf{R}_\eta(N_s) = \frac{1}{N_s} \sum_{n=L-1}^{L-2+N_s} \hat{\eta}(n)\hat{\eta}^\dagger(n), \tag{4.47}$$

$R_\eta(N_s)$ is nearly a Wishart random matrix [41].

For large number of samples, test statistic tends to 1 for $R_\eta(N_s)$ [39]. For the test statistic, we have

Theorem 2. *The test statistic, $\hat{C}_E$, for the sample covariance matrix of the noise, $R_\eta(N_s)$, converges to C_E in mean square sense.*

Proof. The mean squared error from (4.37) and putting values of a_1 from (4.26) and a_2 from (4.27), we get

$$\begin{aligned} E[(C_E - \hat{C}_E)^2] &= E[(\overline{C}_E - a_1\overline{C}_{EL} - a_2\overline{C}_{EU})^2] \\ &= E[(C_E - \mu_C - \frac{\sigma_U^2\sigma_{CL} - \sigma_{LU}\sigma_{CU}}{\sigma_L^2\sigma_U^2 - (\sigma_{LU})^2}(C_{EL} - \mu_L) \\ &\quad - \frac{\sigma_L^2\sigma_{CU} - \sigma_{LU}\sigma_{CL}}{\sigma_L^2\sigma_U^2 - (\sigma_{LU})^2}(C_{EU} - \mu_U))^2] \end{aligned} \tag{4.48}$$

As C_E tends to one for $R_\eta(N_s)$, μ_C also tends to one. Considering this, σ_{CL}, σ_{CU} from (4.44) goes

to zero. Putting all these values in (4.48), we get,

$$E[(C_E - \hat{C}_E)^2] = 0 \tag{4.49}$$

So, $\hat{C}_E$ converges to C_E in the mean square sense. Hence, proved. □

Theorem 2 implies that the decision threshold and probability of detection obtained in [39] holds in our case also and is repeated for convenience. The decision threshold, γ, is given by

$$\begin{aligned}\gamma &= \frac{Q^{-1}(P_{fa})\sqrt{2N_s} + \sqrt{M}N_s}{\sqrt{M}(\sqrt{N_s} - \sqrt{ML})^2} \\ &= \left(\sqrt{\frac{2}{MN_s}}Q^{-1}(P_{fa}) + 1\right)\frac{N_s}{(\sqrt{N_s} - \sqrt{ML})^2}\end{aligned} \tag{4.50}$$

The probability of detection, P_d, is given by

$$P_d = Q\left(\frac{\gamma\left(\rho_{ML} + \frac{\sigma_\eta^2}{\sqrt{N_s}}(\sqrt{N_s} - \sqrt{ML})\right) - \frac{Tr(HR_sH^\dagger)}{ML} - \sigma_\eta^2}{\sqrt{\frac{2}{MN_s}}\sigma_\eta^2}\right) \tag{4.51}$$

where ρ_{ML} is the lowest eigenvalue of $HR_sH^\dagger$.

We know that the sum of the eigenvalues of a matrix is the trace of the matrix. Let m be the average of the eigenvalues of $R_x(N_s)$. Then

$$\begin{aligned}m &= \frac{trace(R_x(N_s))}{ML} \\ &= \frac{1}{MLN_s}\sum_{n=L-1}^{L-2+N_s}\hat{x}^\dagger(n)\hat{x}(n).\end{aligned} \tag{4.52}$$

Simplifying, we get

$$m = \frac{1}{MLN_s}\sum_{i=1}^{M}\sum_{k=0}^{L-2+N_s}\delta(k)|x_i(k)|^2, \tag{4.53}$$

where

$$\delta(k) = \begin{cases} k+1, & 0 \le k \le L-2 \\ L, & L-1 \le k \le N_s - 1 \\ N_s + L - k - 1, & N_s \le k \le N_s + L - 2 \end{cases}$$

Since, N_s is much larger than L, we have

$$m \approx \frac{1}{MN_s}\sum_{i=1}^{M}\sum_{k=0}^{N_s-1}|x_i(k)|^2 = T(N_s). \tag{4.54}$$

Chapter 5

Conclusions and Future Work

We presented dynamic spectrum sharing between the GSM operators. The proposed spectrum sharing algorithm is tested under different traffic conditions by modeling call arrival as independent poisson process. The tremendous increment of 38% in spectrum utilization is observed in two BS co-ordination case when one of BSs having less traffic load. The maximum spectrum efficiency gain of 3.4% in two BS co-ordination and 4.9% in three BS co-ordination is observed when all the BSs in co-ordination having same call arrival rate. ROC gives us an idea about traffic conditions under which co-ordination to be done and how much gain it will provide. Future work will try to address the delays involved in call setup procedure considered with different number of operators and DSS schemes. In future, we will try to do modifications to an existing GSM pricing so that it will be able to support proposed DSS schemes.

References

[1] T. Weiss and F. Jondral. Spectrum pooling: an innovative strategy for the enhancement of spectrum efficiency. *Communications Magazine, IEEE* 42, (2004) 8–14.

[2] D. Willkomm, S. Machiraju, J. Bolot, and A. Wolisz. Primary Users in Cellular Networks: A Large-Scale Measurement Study. In New Frontiers in Dynamic Spectrum Access Networks, 2008. DySPAN 2008. 3rd IEEE Symposium on. 2008 1–11.

[3] K. Patil, K. Skouby, A. Chandra, and R. Prasad. Spectrum occupancy statistics in the context of cognitive radio. In Wireless Personal Multimedia Communications (WPMC), 2011 14th International Symposium on. 2011 1–5.

[4] K. Naidu, Y. Kumar, B. Baveja, R. Naik, B. Sridhar, S. Ponnappa, M. Zafar Ali Khan, S. Merchant, and U. Desai. A Study on White and Gray Spaces in India. In A. K. Mishra and D. L. Johnson, eds., White Space Communication, Signals and Communication Technology, 49–73. Springer International Publishing, 2015.

[5] A. Subramanian and H. Gupta. Fast Spectrum Allocation in Coordinated Dynamic Spectrum Access Based Cellular Networks. In New Frontiers in Dynamic Spectrum Access Networks, 2007. DySPAN 2007. 2nd IEEE International Symposium on. 2007 320–330.

[6] Q. Zhao and B. Sadler. A Survey of Dynamic Spectrum Access. *Signal Processing Magazine, IEEE* 24, (2007) 79–89.

[7] J. Peha. Spectrum management policy options. *Communications Surveys, IEEE* 1, (1998) 2–8.

[8] M. Buddhikot and K. Ryan. Spectrum management in coordinated dynamic spectrum access based cellular networks. In New Frontiers in Dynamic Spectrum Access Networks, 2005. DySPAN 2005. 2005 First IEEE International Symposium on. 2005 299–307.

[9] J. Peha. Approaches to spectrum sharing. *Communications Magazine, IEEE* 43, (2005) 10–12.

[10] I. F. Akyildiz, W.-Y. Lee, M. C. Vuran, and S. Mohanty. NeXt Generation/Dynamic Spectrum Access/Cognitive Radio Wireless Networks: A Survey. *Comput. Netw.* 50, (2006) 2127–2159.

[11] B. Aazhang, J. Lilleberg, and G. Middleton. Spectrum sharing in a cellular system. In Spread Spectrum Techniques and Applications, 2004 IEEE Eighth International Symposium on. 2004 355–359.

[12] G. Salami and R. Tafazolli. Inter-operator Dynamic Spectrum Sharing (Analysis, Cost and Implications). *Int. J. Comput. Netw.* 2, (2010) 47–61.

[13] S. Kumar, G. Costa, S. Kant, F. Frederiksen, N. Marchetti, and P. Mogensen. Spectrum sharing for next generation wireless communication networks. In Cognitive Radio and Advanced Spectrum Management, 2008. CogART 2008. First International Workshop on. 2008 1–5.

[14] J. S. Panchal. Inter-operator resource sharing in 4G LTE cellular networks. Ph.D. thesis, ECE Department, Rutgers University, NJ, 2011 .

[15] V. B. Iversen. Teletraffic Engineering Handbook. Technical University of Denmark.

[16] J. Guo, F. Liu, and Z. Zhu. Estimate the Call Duration Distribution Parameters in GSM System Based on K-L Divergence Method. In Wireless Communications, Networking and Mobile Computing, 2007. WiCom 2007. International Conference on. 2007 2988–2991.

[17] C. Raman, R. Yates, and N. B. Mandayam. Scheduling variable rate links via a spectrum server. In New Frontiers in Dynamic Spectrum Access Networks, 2005. DySPAN 2005. 2005 First IEEE International Symposium on. 2005 110–118.

[18] O. Ileri, D. Samardzija, and N. Mandayam. Demand responsive pricing and competitive spectrum allocation via a spectrum server. In New Frontiers in Dynamic Spectrum Access Networks, 2005. DySPAN 2005. 2005 First IEEE International Symposium on. 2005 194–202.

[19] R. Etkin, A. Parekh, and D. Tse. Spectrum sharing for unlicensed bands. *Selected Areas in Communications, IEEE Journal on* 25, (2007) 517–528.

[20] J. Huang, R. Berry, and M. Honig. Spectrum sharing with distributed interference compensation. In New Frontiers in Dynamic Spectrum Access Networks, 2005. DySPAN 2005. 2005 First IEEE International Symposium on. 2005 88–93.

[21] K. Yuva, M. Saitwal, M. Khan, and U. Desai. Cognitive GSM OpenBTS. In Mobile Ad Hoc and Sensor Systems (MASS), 2014 IEEE 11th International Conference on. 2014 529–530.

[22] J. Mitola and J. Maguire, G.Q. Cognitive radio: making software radios more personal. *Personal Communications, IEEE* 6, (1999) 13–18.

[23] S. Haykin. Cognitive radio: brain-empowered wireless communications. *Selected Areas in Communications, IEEE Journal on* 23, (2005) 201–220.

[24] D. Cabric, S. M. Mishra, D. Willkomm, R. Brodersen, and A. Wolisz. A Cognitive Radio Approach for Usage of Virtual Unlicensed Spectrum. In 14th IST Mobile Wireless Commun. Summit. 2005 .

[25] A. Sahai and D. Cabric. Spectrum sensing: fundamental limits and practical challenges. presented at IEEE International Symp. New Frontiers Dynamic Spectrum Access Networks (DySPAN), Baltimore, MD, 2005 .

[26] A. Sonnenschein and P. Fishman. Radiometric detection of spread-spectrum signals in noise of uncertain power. *Aerospace and Electronic Systems, IEEE Transactions on* 28, (1992) 654–660.

[27] R. Tandra and A. Sahai. Fundamental limits on detection in low SNR under noise uncertainty. In Wireless Networks, Communications and Mobile Computing, 2005 International Conference on, volume 1. 2005 464–469 vol.1.

[28] H. Urkowitz. Energy detection of unknown deterministic signals. *Proceedings of the IEEE* 55, (1967) 523–531.

[29] S. M. Kay. Fundamentals of statistical signal processing: estimation theory. volume 2. Prentice-Hall, 1998 .

[30] FCC. Facilitating opportunities for flexible, efficient, and reliable spectrum use employing cognitive radio technologies, notice of proposed rule making and order. *FCC 03-322* .

[31] 802.22 Working Group. IEEE P802.22/D0.1 Draft Standard for Wireless Regional Area Networks. 2006.

[32] D. Cabric, A. Tkachenko, and R. Brodersen. Spectrum Sensing Measurements of Pilot, Energy, and Collaborative Detection. In Military Communications Conference, 2006. MILCOM 2006. IEEE. 2006 1–7.

[33] H.-S. Chen, W. Gao, and D. Daut. Signature Based Spectrum Sensing Algorithms for IEEE 802.22 WRAN. In Communications, 2007. ICC '07. IEEE International Conference on. 2007 6487–6492.

[34] W. Gardner. Exploitation of spectral redundancy in cyclostationary signals. *Signal Processing Magazine, IEEE* 8, (1991) 14–36.

[35] W. Gardner. Spectral Correlation of Modulated Signals: Part I–Analog Modulation. *Communications, IEEE Transactions on* 35, (1987) 584–594.

[36] W. Gardner, W. Brown, and C.-K. Chen. Spectral Correlation of Modulated Signals: Part II–Digital Modulation. *Communications, IEEE Transactions on* 35, (1987) 595–601.

[37] N. Han, S. Shon, J. H. Chung, and J. M. Kim. Spectral correlation based signal detection method for spectrum sensing in IEEE 802.22 WRAN systems. In Advanced Communication Technology, 2006. ICACT 2006. The 8th International Conference, volume 3. 2006 6 pp.–1770.

[38] S. Shellhammer and R. Tandra. Performance of the Power Detector with Noise Uncertainty. doc. IEEE 802.22-06/0134r0, 2006 .

[39] Y. Zeng and Y.-C. Liang. Eigenvalue-based spectrum sensing algorithms for cognitive radio. *Communications, IEEE Transactions on* 57, (2009) 1784–1793.

[40] H. Wolkowicz and G. P. Styan. Bounds for eigenvalues using traces. *Linear Algebra and its Applications* 29, (1980) 471 – 506. Special Volume Dedicated to Alson S. Householder.

[41] A. M. Tulino and S. Verdú. Random Matrix Theory and Wireless Communications. *Commun. Inf. Theory* 1, (2004) 1–182.